Supporting Information

Step-wise induction, amplification and inversion of molecular chirality through the coordination of chiral diamines with Zn(II)bisporphyrin

Sk. Asif Ikbal, Sanfaori Brahma and Sankar Prasad Rath*

Department of Chemistry, Indian Institute of Technology Kanpur, Kanpur-208016, India

Instrumentation

ESI-MS spectra were recorded on a waters Micromass Quattro Microtriple quadrapole mass spectrometer. ^{1}H NMR spectra were recorded on a JEOL 500 MHz instrument. The residual ^{1}H resonances of the solvents were used as a secondary reference. UV-vis and CD-spectra were recorded on a Perkin-Elmer UV-vis and a JASCO J-815 spectrometer, respectively.

X-ray Structure Solution and Refinement. Single-crystal X-ray data were collected at 100 K on a Bruker SMART APEX CCD diffractometer equipped with CRYO Industries low temperature apparatus and intensity data were collected using graphite-monochromated Mo Kα radiation (λ= 0.71073 Å). The data integration and reduction were processed with SAINTsoftware.[1] An absorption correction was applied.[2] The structure was solved by the direct methodusing SHELXS-97 and was refined on F2 by full-matrix least-squares technique using the SHELXL-2014 program package.[3] Non-hydrogen atoms were refined anisotropically. In the refinement, hydrogens were treated as riding atoms using SHELXL default parameters.

Computational Details.

DFT calculations have been carried out by employing two different methods, OPBE/LANL2TZ level and PM3 semi-empirical method using the Gaussian 09, revision B.01, package.[4] Single point energy calculations are performed by gradient corrected correlational functional OPBE.[5] The basis set was 6-31G+ for carbon, nitrogen and hydrogen atoms. Single point energy calculations of both the oligomers were carried out in dichloromethane solvent taking the coordinates from the crystal structure of $\mathbf{1}_2$•[(1*S*, 2*S*)-CHDA]$_3$. Geometry optimizations are also done in gas phase on both the

oligomers separately using PM3 semi-empirical method[6] taking the coordinates from the crystal structure of $\mathbf{1}_2$•[(1*S*, 2*S*)-CHDA]$_3$.

Experimental:

Materials:

The zinc-complex of diethylpyrrole-bridged bisporphyrin, **1**, has been synthesized following the reported procedure.[7] Reagents and solvents are purchased from commercial sources and purified by standard procedures before use. Enantiomerically pure (1*S*, 2*S*)-cyclohexane diamine, (*S*)-2-aminobutane, (*R*)-1-phenyl-ethylamine, achiral cyclohexylamine were purchased from Sigma-Aldrich while enatiomerically pure (*S*)-3-phenylpropane-1,2-diamine has been synthesized by the following procedure.[8]

Synthesis of 1•(1*S*, 2*S*)-CHDA

Compound **1** (50 mg, 0.037 mmol) was dissolved in $CHCl_3$ (5 mL). 4 mg (0.035 mmol) of (1*S*, 2*S*)-CHDA was added to it and stirred for about 30 min. The solution obtained was then filtered off to remove any solid residue and carefully layered with acetonitrile at room temperature. On standing for 6-7 days purple square shaped crystals were grown, which was then isolated by filtration, washed well with n-hexane, and dried well in vacuum. Yield 28 mg (52%). UV-vis (CH_2Cl_2) [λ_{max}, nm (ε, M^{-1} cm^{-1})]: 412 (3.1×10^5), 549 (2.4×10^4), 585 (1.2×10^4). ESI-MS: *m*/*z* 1454.8005 ($[M+H]^+$).

Synthesis of $\mathbf{1}_2$•[(1*S*, 2*S*)-CHDA]$_3$

Compound **1** (50 mg, 0.037 mmol) was dissolved in $CHCl_3$ (5 mL). 51 mg (0.44 mmol) of (1*S*, 2*S*)-CHDA was added to it and stirred for about 30 min. The solution obtained was then filtered off to remove any solid residue and carefully layered with acetonitrile at room temperature. On standing for 6-7 days purple needle shaped crystals were grown, which was then isolated by filtration, washed well with n-hexane, and dried well in vacuum. Yield 34 mg (60%). UV-vis (CH_2Cl_2) [λ_{max}, nm (ε, M^{-1} cm^{-1})]: 413 (3.0×10^5), 550 (2.2×10^4), 586 (1.0×10^3).

Synthesis of 1•(*S*)-PPDA

Compound **1** (50 mg, 0.037 mmol) was dissolved in $CHCl_3$ (5 mL). 5 mg (0.033 mmol) of (*S*)-PPDA was added to it and stirred for about 30 min. The solution obtained was then filtered off to remove any solid residue and carefully layered with acetonitrile at room temperature. On standing for 6-7

days reddish solid precipitated out, which was then isolated by filtration, washed well with n-hexane, and dried well in vacuum. Yield 35 mg (63%). UV-vis (CH_2Cl_2) [λ_{max}, nm (ε, M^{-1} cm^{-1})]: 412 (3.2×10^5), 550 (2.2×10^4), 587 (1.0×10^4). ESI-MS: *m*/*z* 1490.7858 ($[M+H]^+$).

Synthesis of 1_2•[(S)-PPDA]$_3$

Compound **1** (50 mg, 0.037 mmol) was dissolved in $CHCl_3$ (5 mL). 61 mg (0.40 mmol) of (*S*)-PPDA was added to it and stirred for about 30 min. The solution obtained was then filtered off to remove any solid residue and carefully layered with acetonitrile at room temperature. On standing for 6-7 days reddish solid precipitated out, which was then isolated by filtration, washed well with n-hexane, and dried well in vacuum. Yield 29 mg (50%). UV-vis (CH_2Cl_2) [λ_{max}, nm (ε, M^{-1} cm^{-1})]: 413 (3.1×10^5), 551 (2.4×10^4), 587 (1.2×10^4).

References

[1] SAINT+, 6.02 ed., Bruker AXS, Madison, WI, **1999**.

[2] Sheldrick, G.M. SADABS 2.0, **2000**.

[3] Sheldrick, G. M. *SHELXL-2014: Program for Crystal Structure Refinement*; University of Göttingen: Göttingen, Germany, **2014**.

[4] Frisch, M.J.; Trucks, G. W.; Schlegel, H. B.; Scuseria, G. E.; Robb, M. A.; Cheeseman, J. R.; Scalmani, G.; Barone, V.; Mennucci, B.; Petersson, G. A.; Nakatsuji, H.; Caricato, M.; Li, X.; Hratchian, H. P.; Izmaylov, A. F.; Bloino, J.; Zheng, G.; Sonnenberg, J. L.; Hada, M.; Ehara, M.; Toyota, K.; Fukuda, R.; Hasegawa, J.; Ishida, M.; Nakajima, T.; Honda, Y.; Kitao, O.; Nakai, H.; Vreven, T.; Montgomery, Jr., J. A.; Peralta, J. E.; Ogliaro, F.; Bearpark, M.; Heyd, J. J.; Brothers, E.; Kudin, K. N.; Staroverov, V. N.; Keith, T.; Kobayashi, R.; Normand, J.; Raghavachari, K.; Rendell, A.; Burant, J. C.; Iyengar, S. S.; Tomasi, J.; Cossi, M.; Rega, N.; Millam, J. M.; Klene, M.; Knox, J. E.; Cross, J. B.; Bakken, V.; Adamo, C.; Jaramillo, J.; Gomperts, R.; Stratmann, R. E.; Yazyev, O.; Austin, A. J.; Cammi, R.; Pomelli, C.; Ochterski, J. W.; Martin, R. L.; Morokuma, K.; Zakrzewski, V. G.; Voth, G. A.; Salvador, P.; Dannenberg, J. J.; Dapprich, S.; Daniels, A. D.; Farkas, O.; Foresman, J. B.; Ortiz, J. V.; Cioslowski, J.; and Fox, D. J. Gaussian, Inc., Wallingford CT, 2010.

[5] (a) Perdew, J. P.; Bruke, K.; Ernerhof, M. *Phys. Rev. Lett.* **1997**, *78*, 1396. (b) Perdew, J. P.; Bruke, K.; Ernerhof, M. *Phys. Rev. Lett.* **1996**, 77, 3865.

[6] (a) Stewart, James J. P. *J. Comput. Chem.* **1989**, *10*, 209. (b) Stewart, James J. P. *J. Comput. Chem.* **1989**, *10*, 221.

[7] Yashunsky, D. V.; Arnold, D.P.; Ponomarev, G. V. *Chem. Heterocycl. Comp.* **2000**, *36*, 275.

[8] Belokon, Y. N.; Pritula, L. K.; Tararov, V. I.; Bakhmutov, V. I.; Struchkov, Y. T.; Timofeeva, T. V.; Belikov, V. M. *J. Chem. Soc*, *Dalton Trans.* **1990**, 1867.

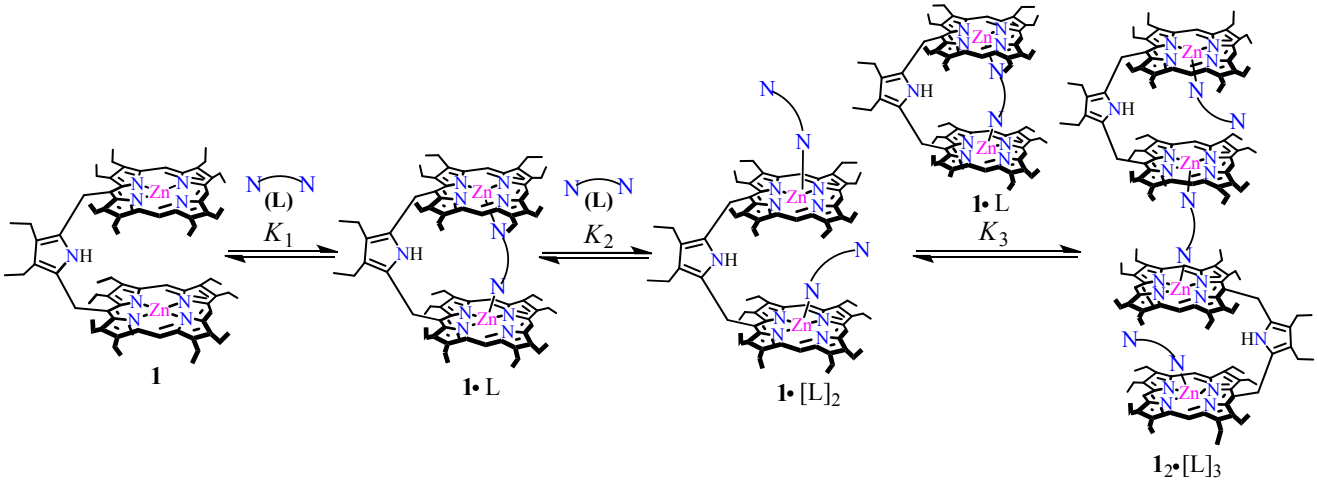

Scheme S1. Schematic representation of the species involved in the equilibrium of binding diamine guest to Zn(II)-bsiporphyrin, **1**. K_1, K_2, K_3 are stepwise binding constants.

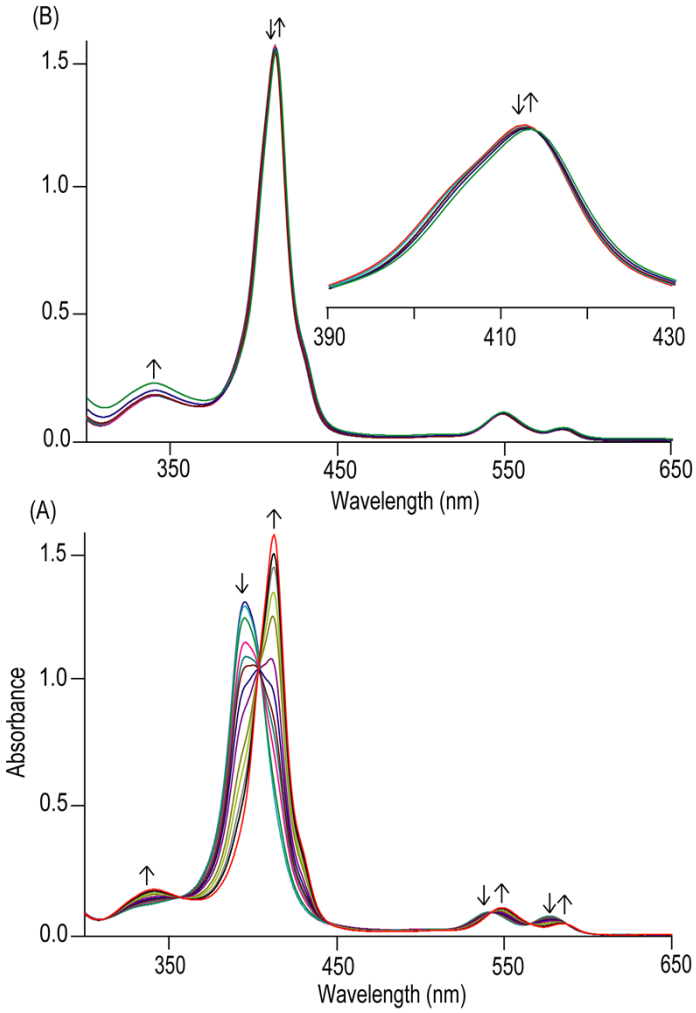

Figure S1. UV-visible (in CH_2Cl_2 at 295 K) spectral change of **1** (at 5 x 10^{-6} M at 10mm path cell) upon addition of (*S*)-PPDA as the host-guest molar ratio change from (A) 1:0 to 1:14 and (B) 1:20 to 390. Inset shows the expanded Soret band region.

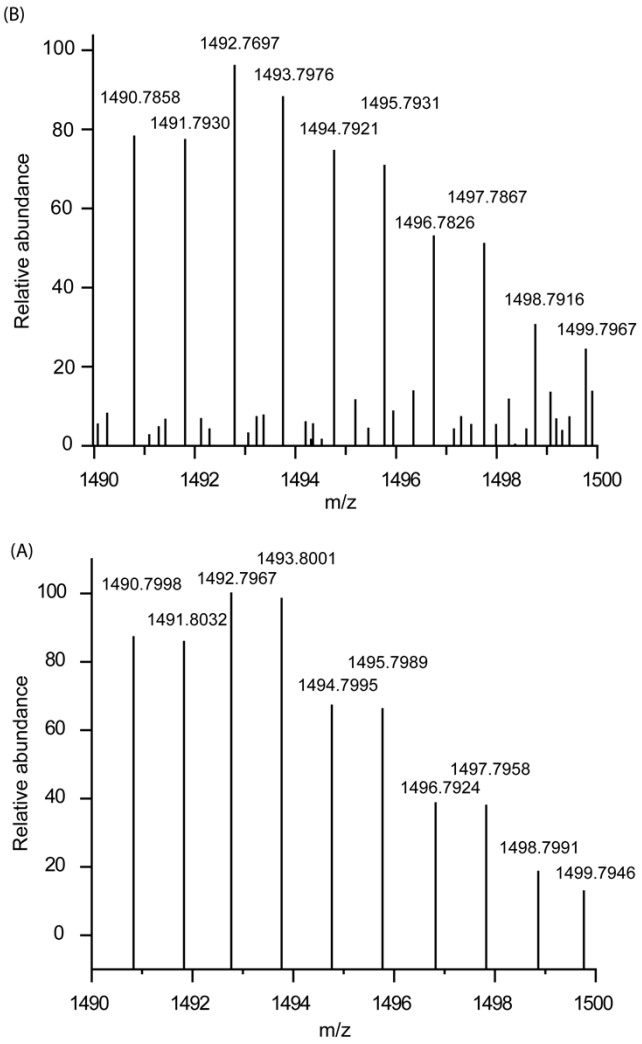

Figure S2. Isotopic distribution pattern (A) theoretical and (B) experimental of ESI-MS of [**1**•(*S*)-PPDA +H]$^+$.

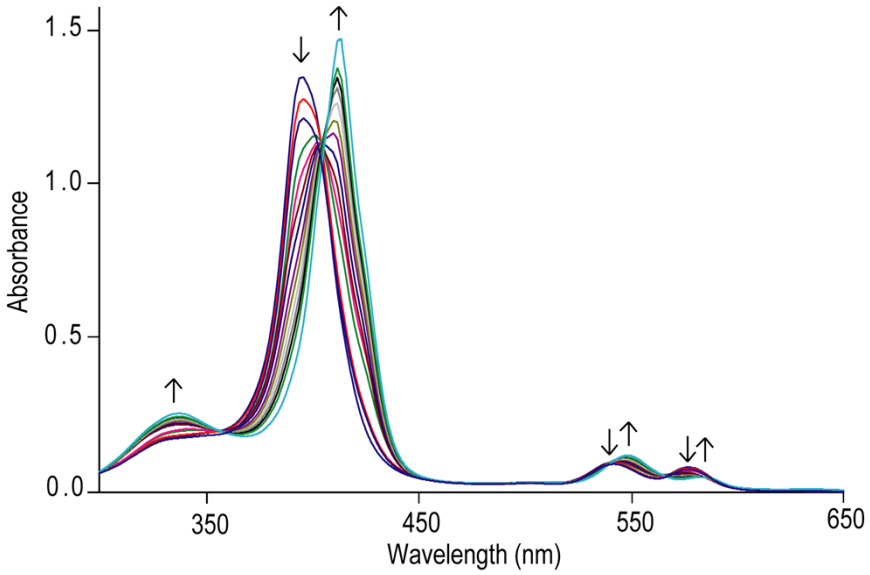

Figure S3. UV-visible (in CH_2Cl_2 at 295 K) spectral change of **1** (at 5 x 10^{-6} M at 10mm path cell) upon addition of (*S*)-2-aminobutane as the host-guest molar ratio change from 1:0 to 1:900.

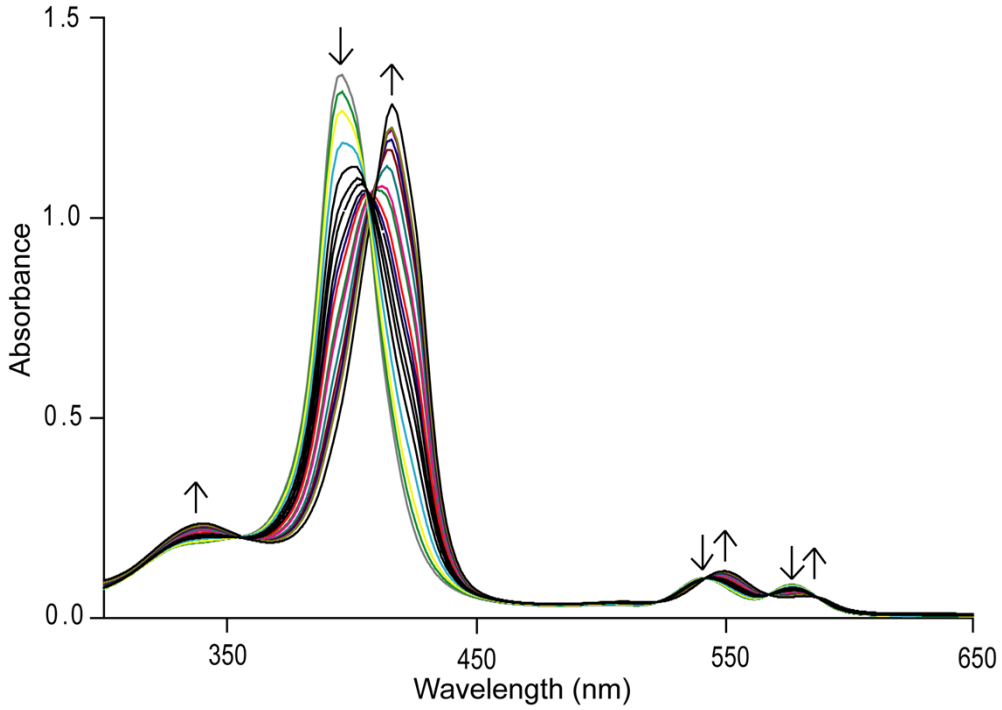

Figure S4. UV-visible (in CH_2Cl_2 at 295 K) spectral change of **1** (at 5 x 10^{-6} M at 10mm path cell) upon addition of (*R*)-1-Ph-ethylamine as the host-guest molar ratio change from 1:0 to 1:1450.

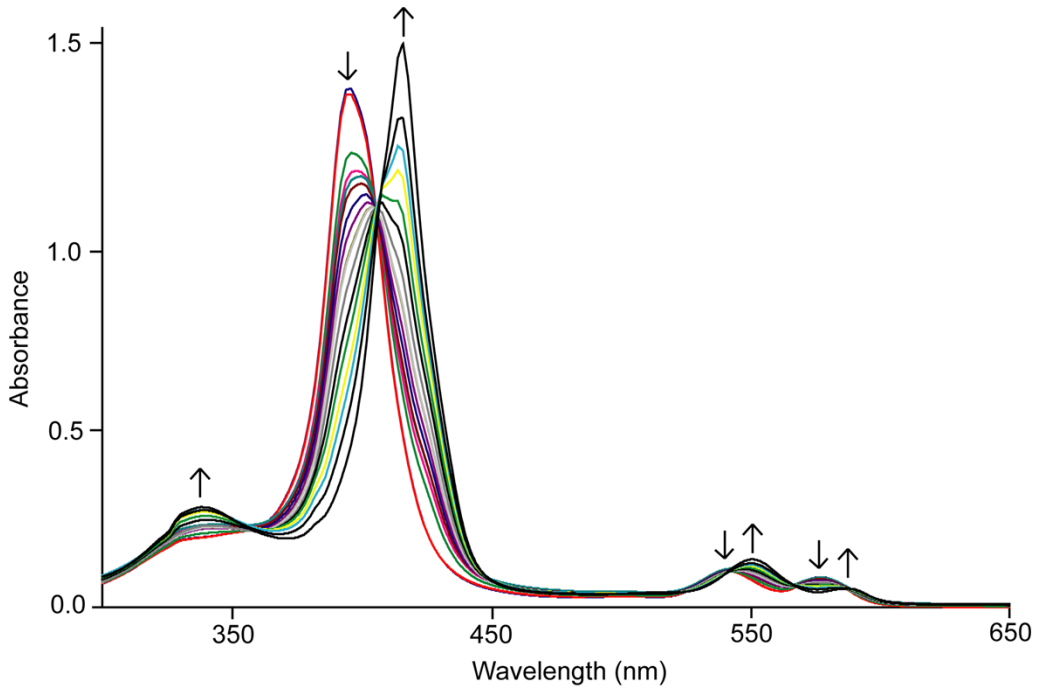

Figure S5. UV-visible (in CH_2Cl_2 at 295 K) spectral change of **1** (at 5 x 10^{-6} M at 10mm path cell) upon addition of cyclohexylamine as the host-guest molar ratio change from 1:0 to 1:750.

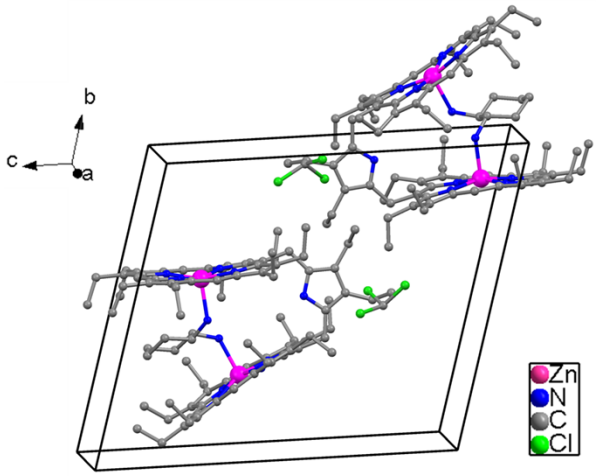

Figure S6. Diagram illustrating the packing of **1**•(1*S*, 2*S*)-CHDA in the unit cell (H atoms have been omitted for clarity).

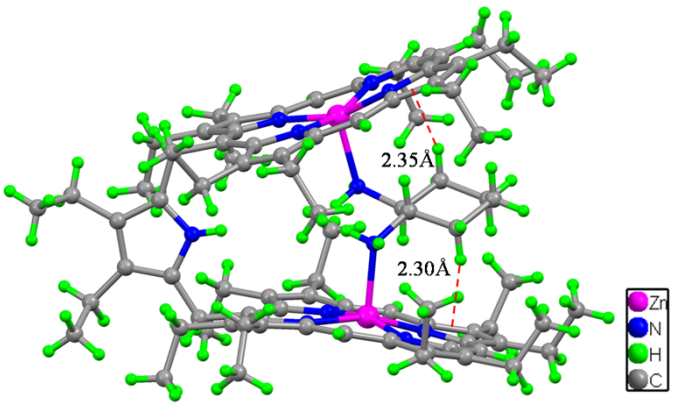

Figure S7. CH-л interaction of ligand hydrogens with the porphyrin pyrrole rings in **1**•(1*S*, 2*S*)-CHDA.

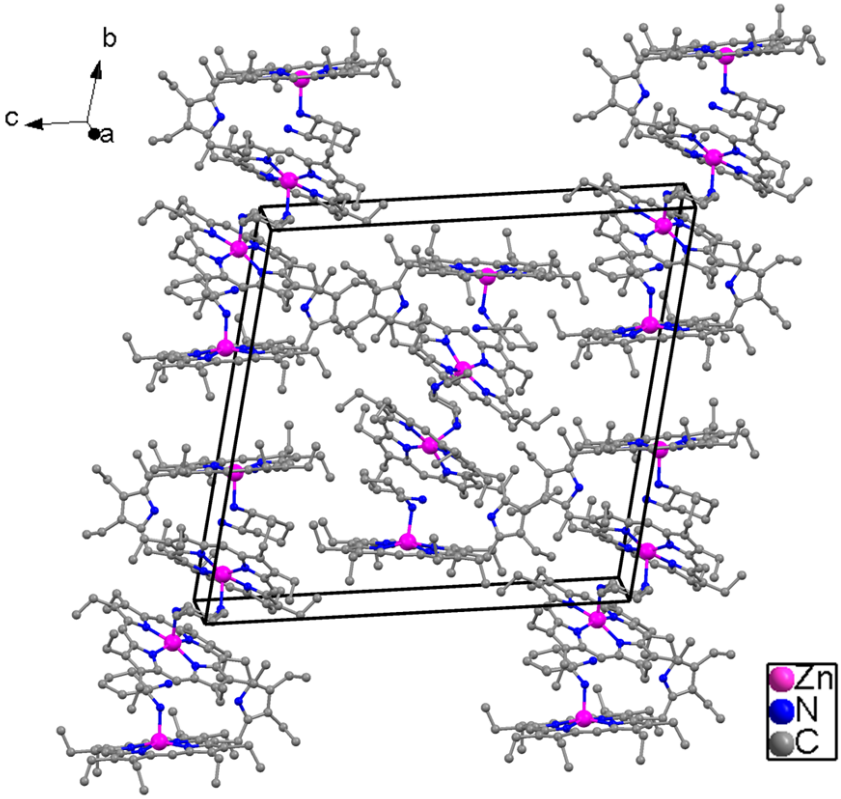

Figure S8. Diagram illustrating the packing of $\mathbf{1}_2$•[(1*S*, 2*S*)-CHDA]$_3$ in the unit cell (H atoms have been omitted for clarity).

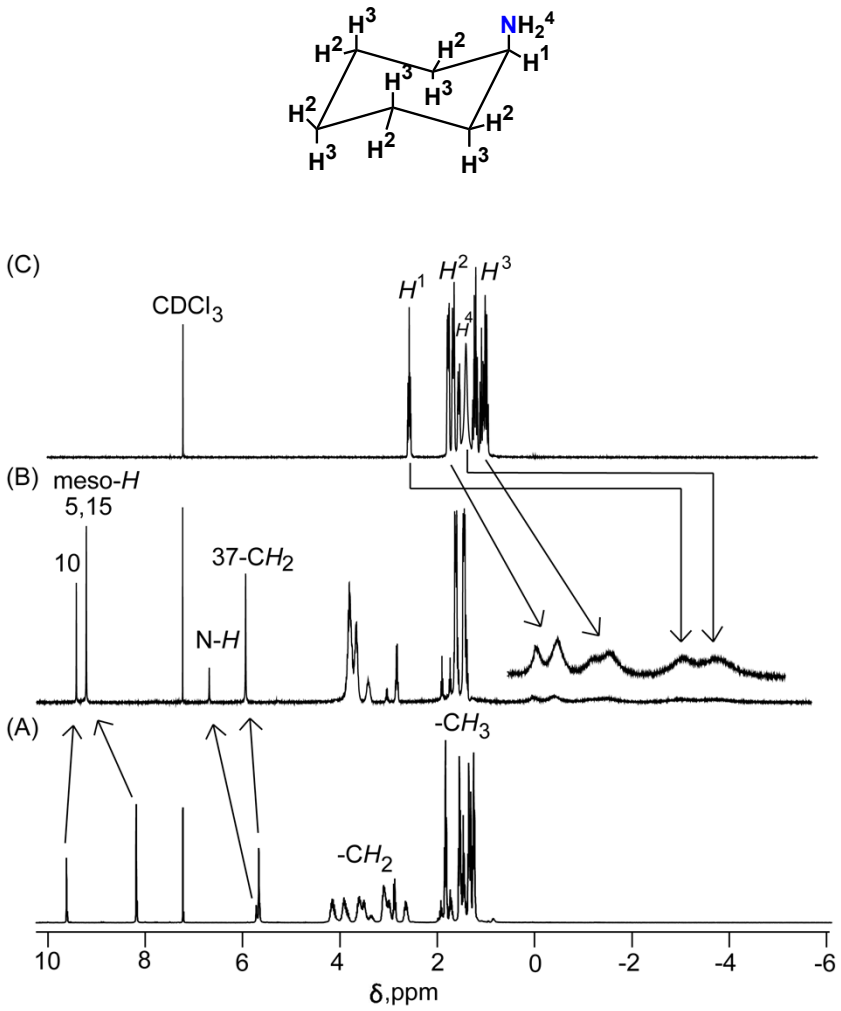

Figure S9. ^{1}H NMR spectra in $CDCl_3$ at 295K of (A) **1** (~10^{-3} M), (B) after addition of 2.0 equivalent of cyclohexylamine and (C) free cyclohexylamine ligand.

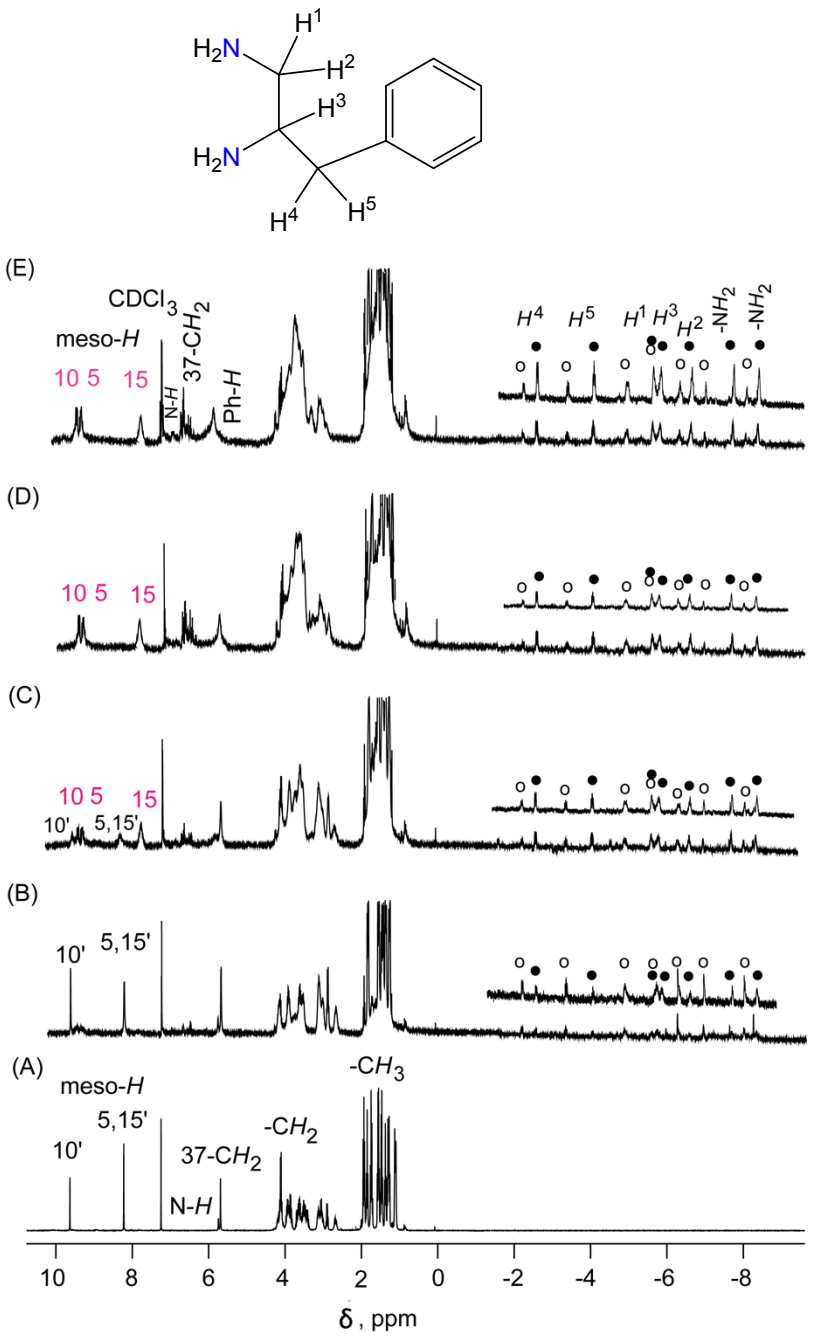

Figure S10. ^{1}H NMR spectral changes of **1** (~10^{-3} M) upon addition of (*S*)-PPDA in $CDCl_3$ at 295 K as the host-guest molar ratio (A) 1 :0, (B) 1 : 0.5, (C) 1 : 1.0, (D) 1 : 1.5, (E) 1 : 2.0. The ratios **1**•(*S*)-PPDA (o) : $\mathbf{1}_2$•[(*S*)-PPDA]$_3$ (●) were (B) 1:0.20, (C) 1:0.45, (D) 1:0.60 and (E) 1:0.80, determined by deconvolution of the peak profiles. Meso-*H* signal for unbound bisporphyrin (10', 5,15') and bound bisporphyrin (10, 5, 15) are shown separately. Inset shows the proton numbering scheme of (*S*)-PPDA.

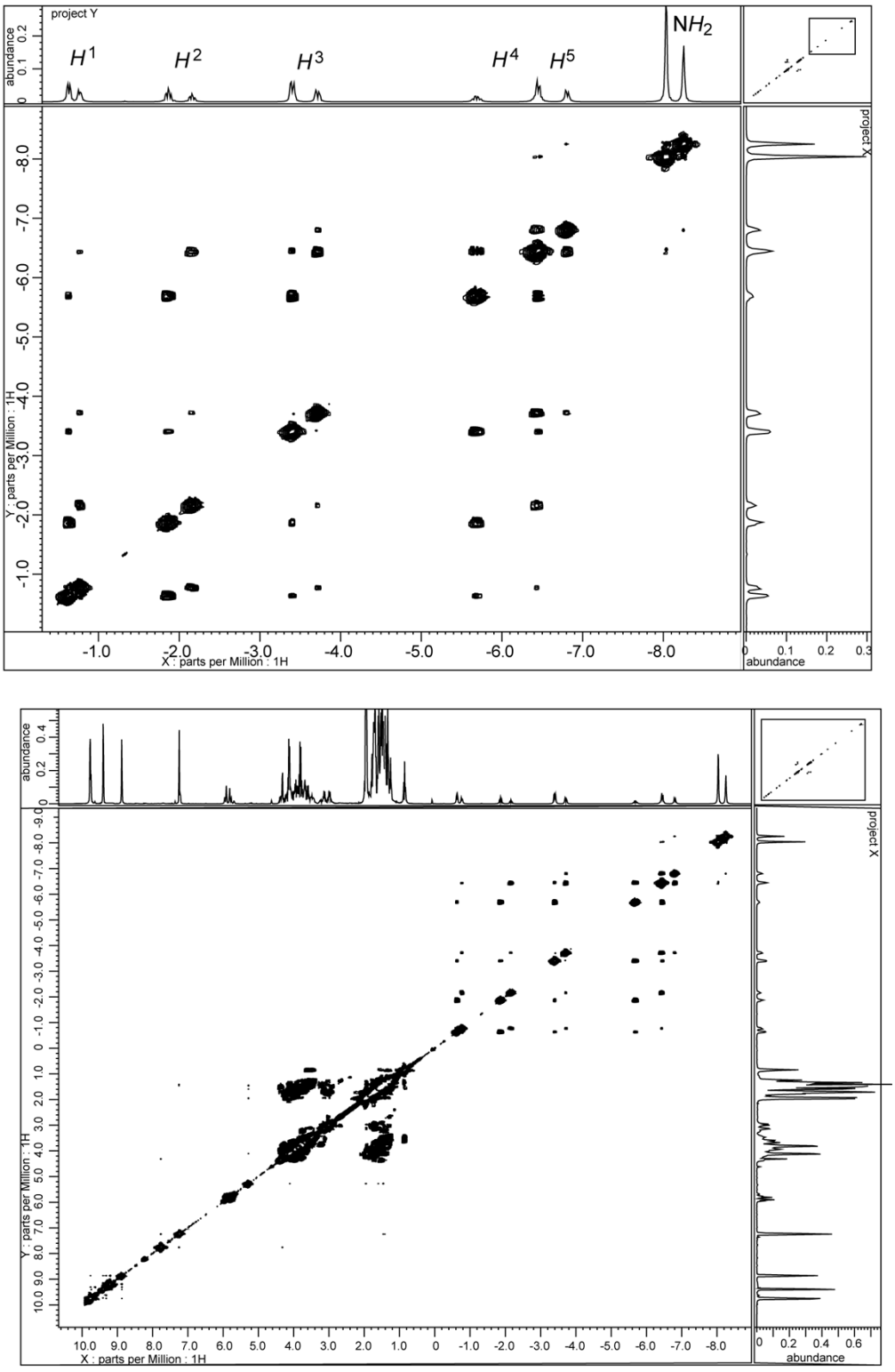

Figure S11. ^{1}H-^{1}H COSY spectrum of polycrystalline sample of **1**•(1*S*, 2*S*)-CHDA in $CDCl_3$ at 295 K. Inset shows the magnified negative region.

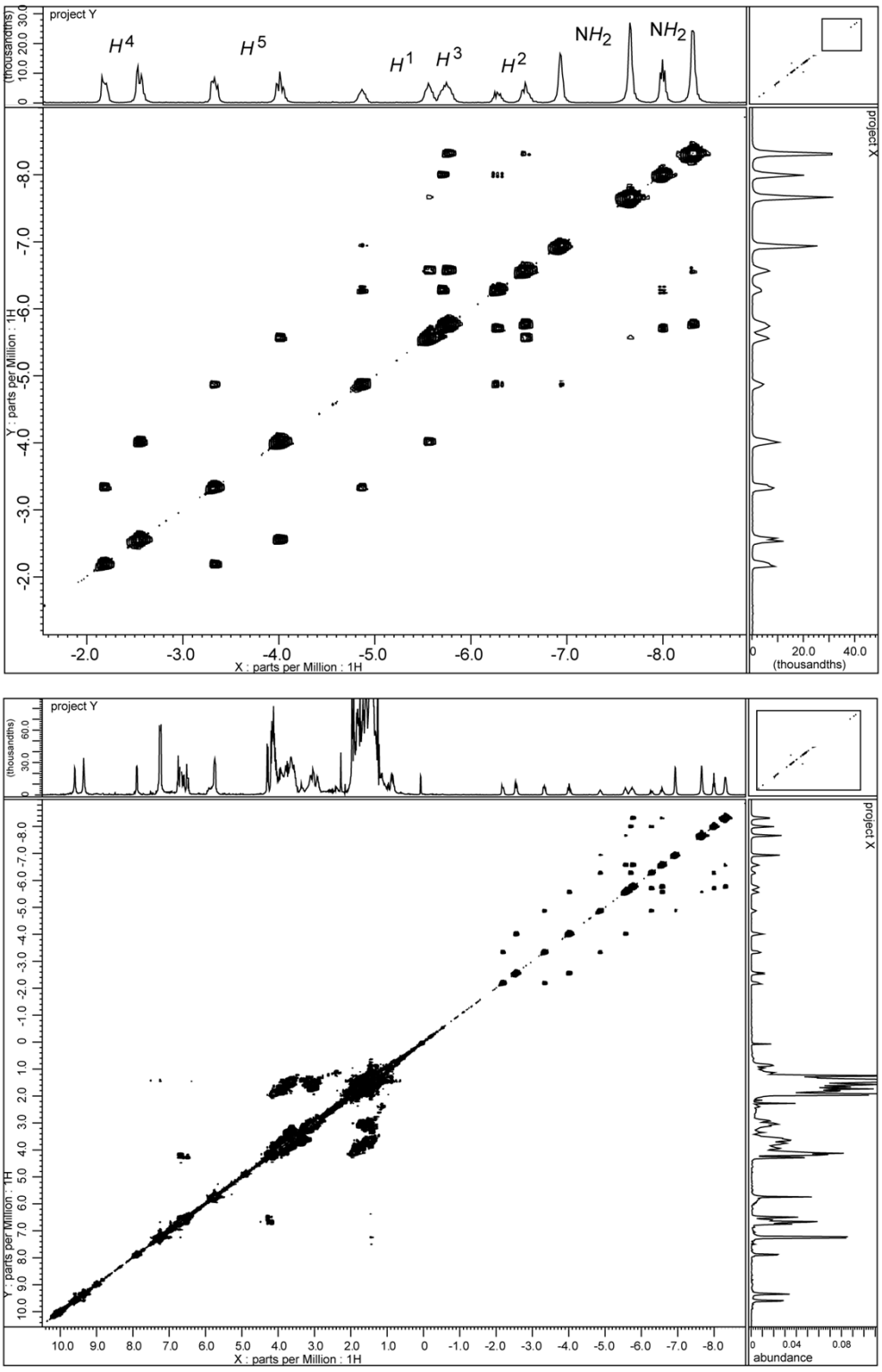

Figure S12. ^{1}H-^{1}H COSY spectrum of polycrystalline sample of $\mathbf{1}_2$•[(*S*)-PPDA]$_3$ in $CDCl_3$. Inset shows the magnified negative region.

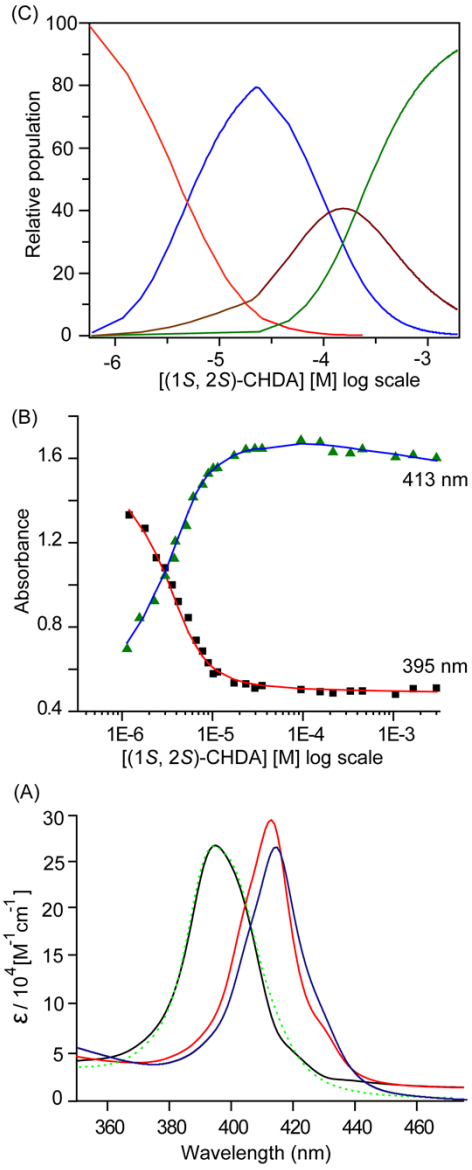

Figure S13. (A) Calculated UV-visible spectra of (black) **1**, (red) **1**•(1*S*, 2*S*)-CHDA and (blue) $\mathbf{1}_2$•[(1*S*, 2*S*)-CHDA]$_3$. Green dotted line represents the observed UV-vis spectra of **1**. (B) Fits of UV titration data of **1** (at 5×10^{-6} M) with (1*S*, 2*S*)-CHDA at selected wavelengths of 413 and 395 nm in CH_2Cl_2 at 295 K. (C) Species distribution plot of the (red line) **1**, (blue line)**1**•(1*S*, 2*S*)-CHDA, (brown line) **1**•[(1*S*, 2*S*)-CHDA]$_2$ and (green line) $\mathbf{1}_2$•[(1*S*, 2*S*)-CHDA]$_3$ complexes.

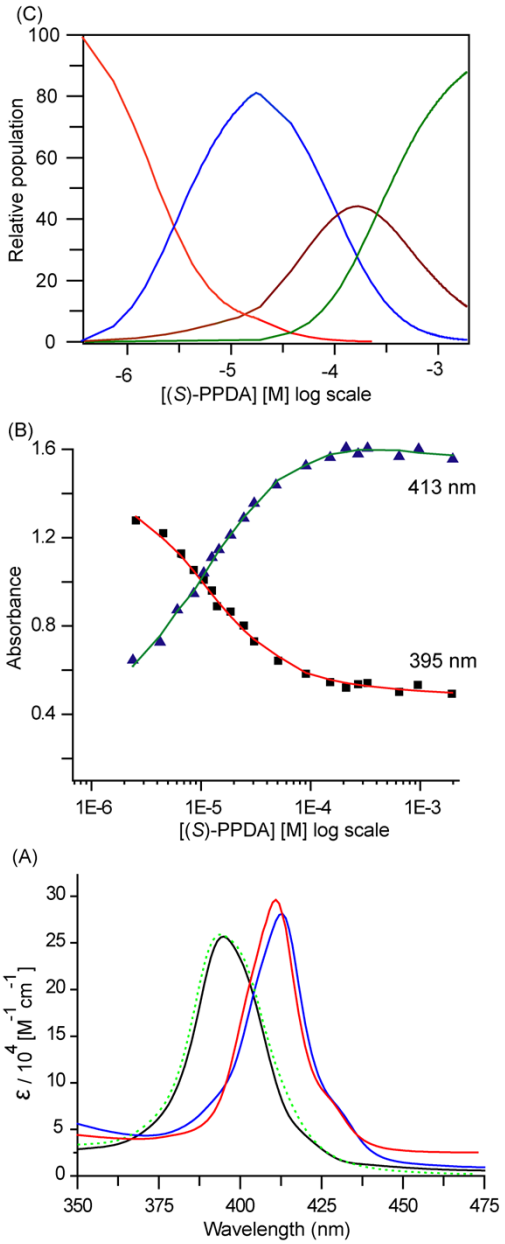

Figure S14. (A) Calculated UV-visible spectra of (black) **1**, (red) **1**•(*S*)-PPDA and (blue) $\mathbf{1}_2$•[(*S*)-PPDA]$_3$. Green dotted line represents the observed UV-vis spectra of **1**. (B) Fits of UV titration data of **1** (at 5×10^{-6} M) with (*S*)-PPDA at selected wavelengths of 413 and 395 nm in CH_2Cl_2 at 295 K. (C) Species distribution plot of the (red line)**1**, (blue line)**1**•(*S*)-PPDA, (brown line) **1**•[(*S*)-PPDA]$_2$ and (green line) $\mathbf{1}_2$•[(*S*)-PPDA]$_3$ complexes.

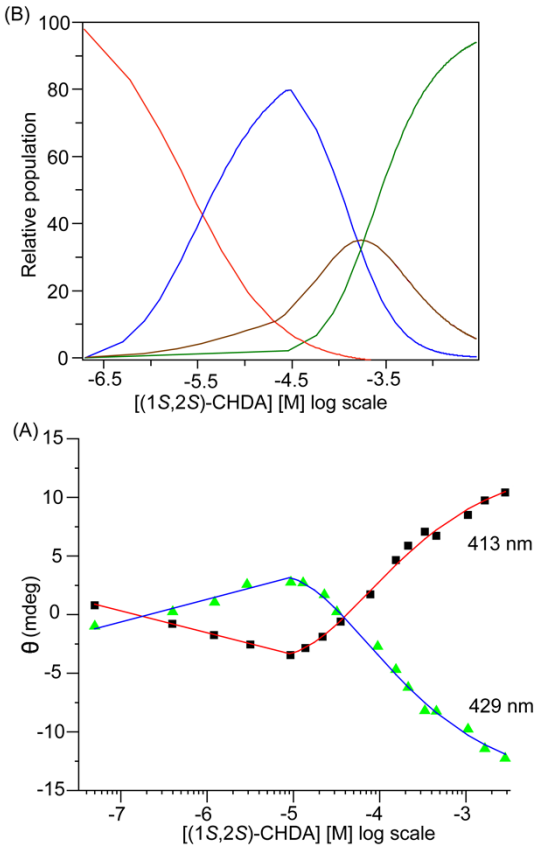

Figure S15. (A) Fits of CD titration data of **1** (at 5 × 10^{-6} M) with (1*S*, 2*S*)-CHDA at selected wavelengths of 413 and 429 nm in CH_2Cl_2 at 295 K. (B) Species distribution plot of the (red line)**1**, (blue line)**1**•(1*S*, 2*S*)-CHDA, (brown line) **1**•[(1*S*, 2*S*)-CHDA]$_2$ and (green line) **1**$_2$•[(1*S*, 2*S*)-CHDA]$_3$ complexes.

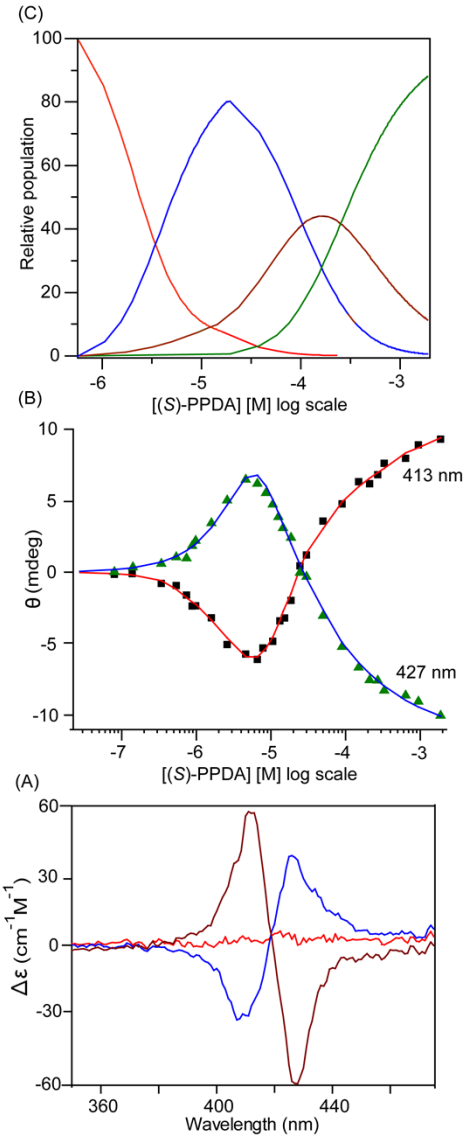

Figure S16. (A) Calculated CD spectra of (red) **1**, (blue) **1**•(*S*)-PPDA and (brown) $\mathbf{1}_2$•[(*S*)-PPDA]$_3$. (B) Fits of CD titration data of **1** (at 5×10^{-6} M) with (*S*)-PPDA at selected wavelengths of 413 and 427 nm in CH_2Cl_2 at 295 K. (C) Species distribution plot of the (red line)**1**, (blue line)**1**•(*S*)-PPDA, (brown line) **1**•[(*S*)-PPDA]$_2$ and (green line) $\mathbf{1}_2$•[(*S*)-PPDA]$_3$ complexes.

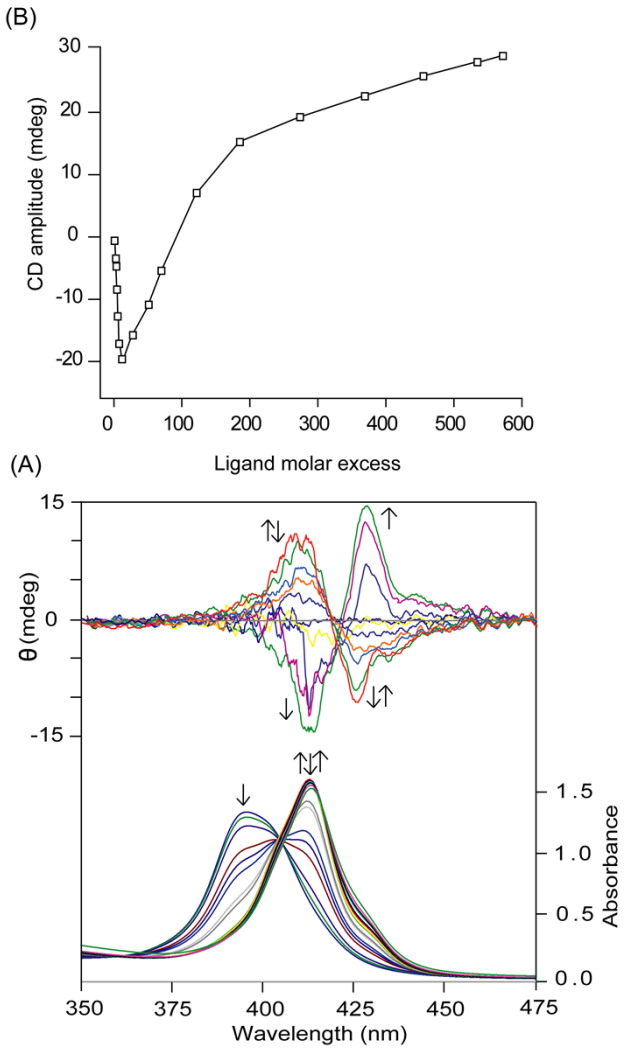

Figure S17. (A) CD and UV-visible spectral changes upon addition of (1*R*, 2*R*)-CHDA to the CH_2Cl_2 solution of **1** (5×10^{-6} M at 10mm path cell) at 295 K as the host: guest molar ratio changes from 1:0 to 1:558. (B) CD amplitude change with substrate molar excess.

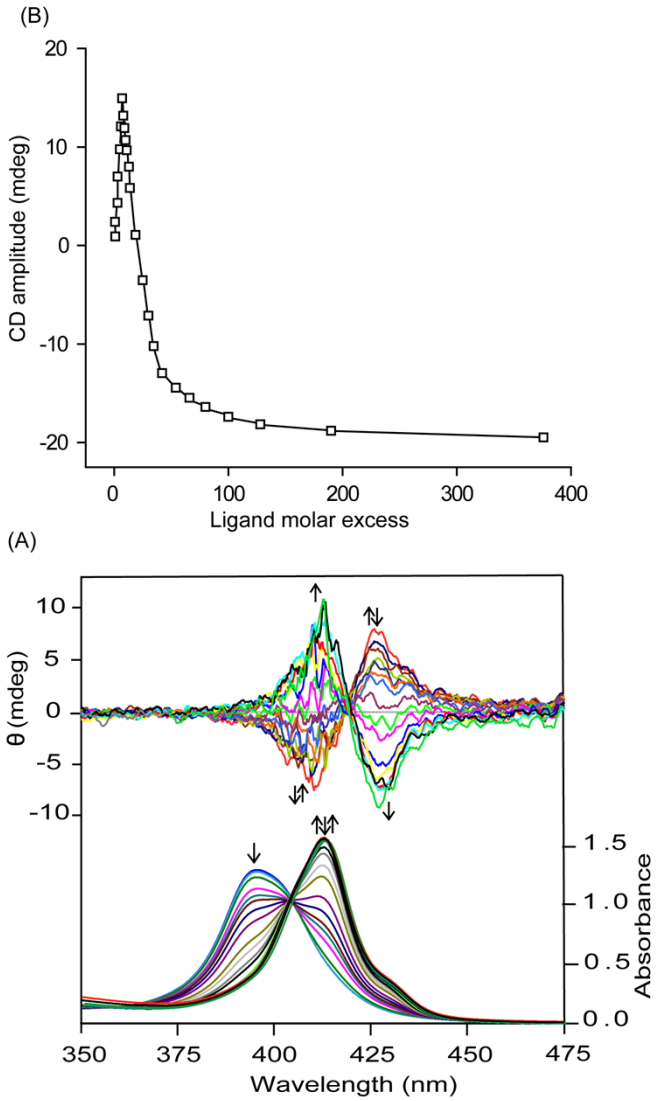

Figure S18. CD and UV-visible spectral changes upon addition of (*S*)-PPDA to the CH_2Cl_2 solution of **1** (5×10^{-6} M at 10mm path cell) at 295 K as the host: guest molar ratio changes from 1:0 to 1:376. (B) CD amplitude change.

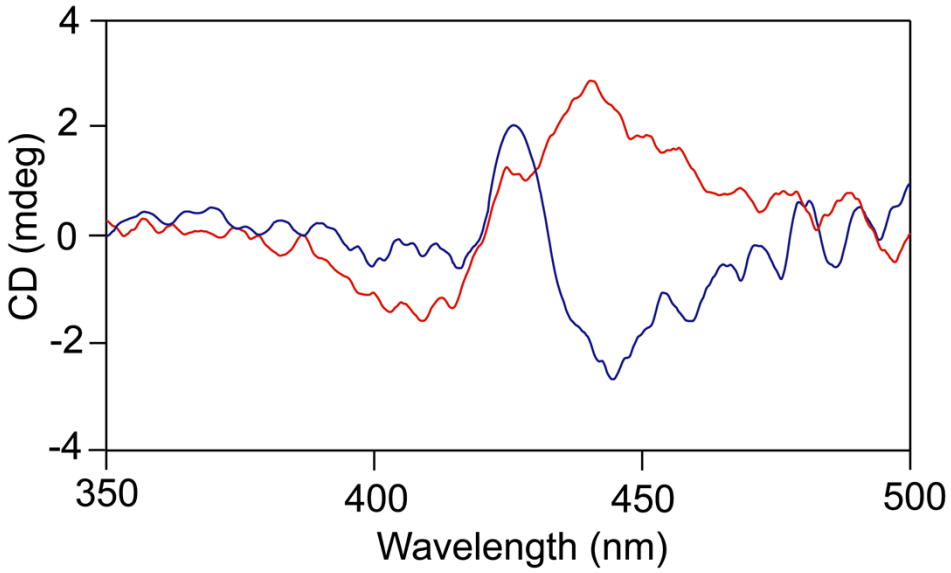

Figure S19. Solid state CD spectra from crystals of **1**•(1*S*,2*S*)-CHDA (red) and $\mathbf{1}_2$•[(1*S*,2*S*)-CHDA]$_3$ (blue) in KBr matrix at 295 K.

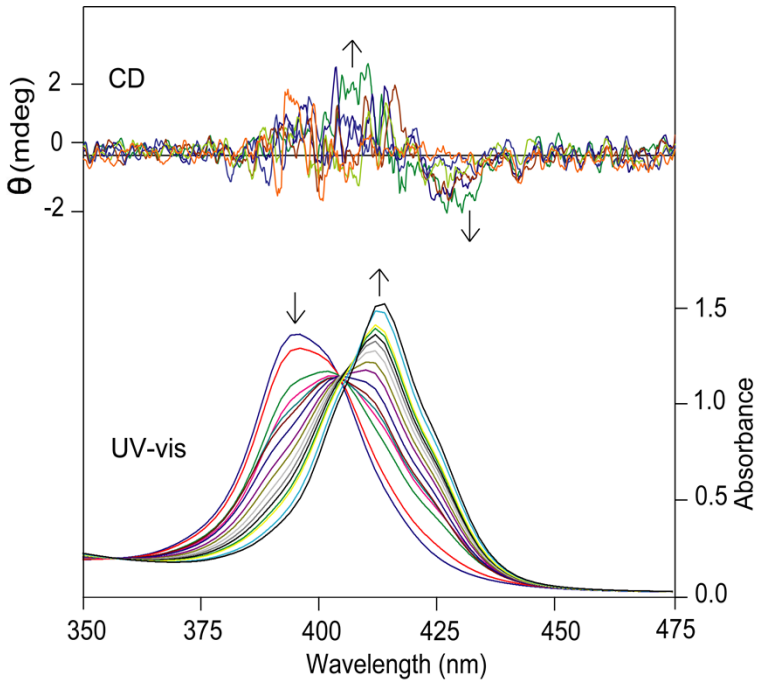

Figure S20. CD and UV-visible spectral change of **1** (5×10^{-6} M at 10mm path cell) in CH_2Cl_2 at 295 K upon gradual addition of (*S*)-2-aminobutane as the host-guest ratio changes from 1:0 to 1:870.

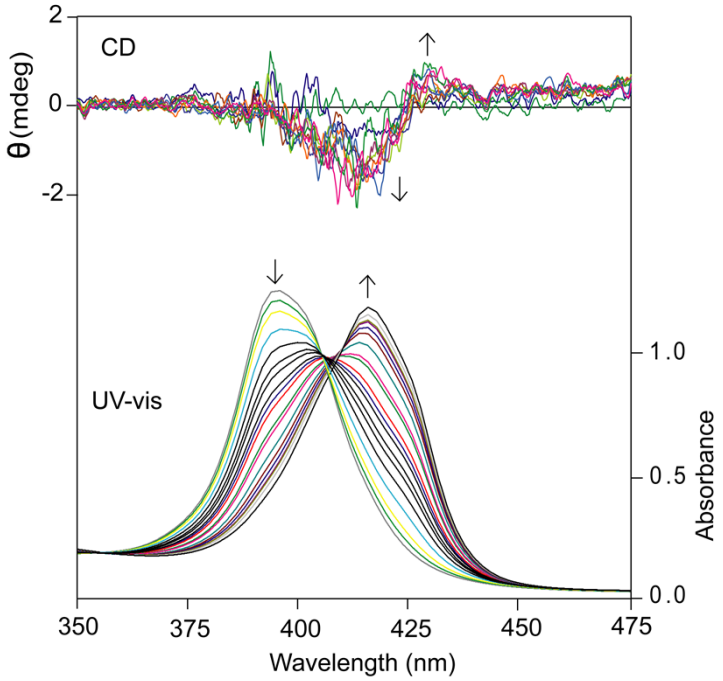

Figure S21. CD and UV-visible spectral change of **1** (5×10^{-6} M at 10mm path cell) in CH_2Cl_2 at 295 K upon gradual addition of (*R*)-1-Ph-ethylamine as the host-guest ratio changes from 1:0 to 1:1380.

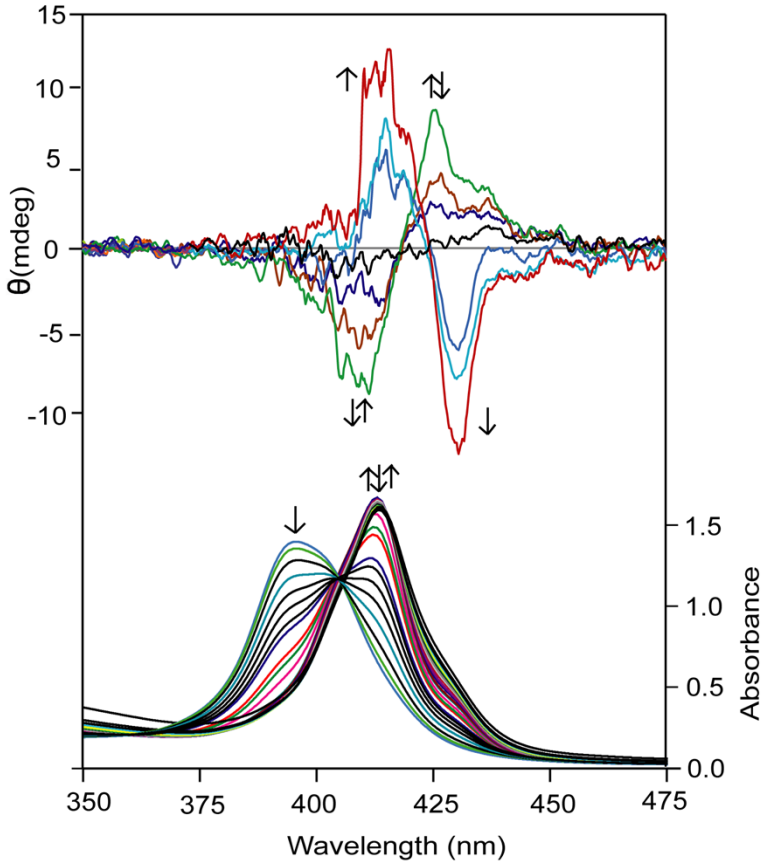

Figure S22. CD and UV-visible spectral change of **1** (5×10^{-5} M at 1mm path cell) in CH_2Cl_2 at 295 K upon gradual addition of (1*S*,2*S*)-CHDA as the host-guest ratio changes from 1:0 to 1:320.

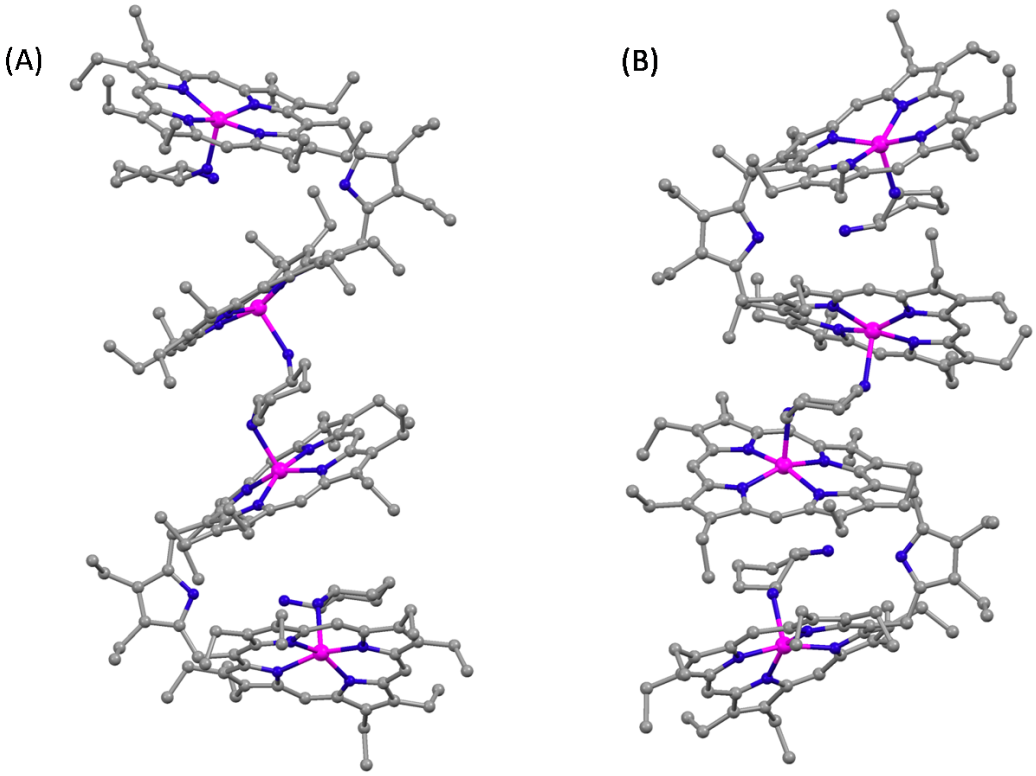

Figure S23. DFT-optimized structures of $\mathbf{1}_2$•[(1*S*,2*S*)-CHDA]$_3$ (A) Anticlockwise, (B) Clockwise components (H-atoms have been removed for clarity).

Table S1. Crystal data and data collection parameters.

	1•(1*S*, 2*S*)-CHDA	$\mathbf{1}_2$•[(1*S*, 2*S*)-CHDA]$_3$
Formula	C_{89} H_{116} Cl_3 N_{11} Zn_2	C_{368} H_{502} $Cl_{18}N_{48}$ O_3Zn_8
T, (K)	100(2)	100(2)
Formula weight	1577.02	6452.71
Crystal system	Triclinic	Monoclinic
Space group	*P*1	*P*2
a, Å	13.469(5)	24.8760(15)
b, Å	16.818(5)	13.2663(7)
c, Å	19.323(5)	26.3877(15)
α , deg	105.183(5)	90
β, deg	100.695(5)	102.292(2)
γ, deg	100.481(5)	90
V, Å^3	4026(2)	8508.6(8)

Radiation (λ, Å)	Mo Kα (0.71073)	Mo Kα (0.71073)
Z	2	1
d_{calcd}, g.cm^{-3}	1.301	1.259
F(000)	1676	3446
μ, mm^{-1}	0.748	0.680
No. of unique data	20101	28953
No. of parameters, refined	1927	1955
GOF on F^2	0.955	0.940
$R1^a$ [$I > 2\sigma(I)$]	0.0587	0.0731
$R1^a$ (all data)	0.1205	0.1289
$wR2^b$ (all data)	0.1176	0.1738

$$a\ R1 = \frac{\sum ||Fo| - |Fc||}{\sum |Fo|}; \quad b\ wR2 = \sqrt{\frac{\sum \left[w\left(Fo^2 - Fc^2\right)^2\right]}{\sum \left[w\left(Fo^2\right)^2\right]}}$$

Table S2: Selected structural parameters

Complex			Zn-N_p[a]	Zn-N_{ax}[a]	Δ^{Zn}_{24}[b]	Δ_{24}[c]	Zn•••Zn[d]	Dihedral angel (θ)[e]	Torsional angel(Φ)[f]
1•(1*S*, 2*S*)-CHDA	molecule-I	Core-I	2.062(6)	2.202(5)	0.33	0.13	6.00	28.6	23.75
		Core-II	2.069(5)	2.218(6)	0.33	0.09			
	molecule-II	Core-I	2.053(6)	2.210(6)	0.30	0.15	6.06	27.7	26.89
		Core-II	2.063(6)	2.229(6)	0.34	0.13			
1$_2$•[(1*S*, 2*S*)-CHDA]$_3$	molecule-I	Core-I	2.082(8)	2.155(8)	0.46	0.05	6.13	38.3	-4.72
		Core-II	2.070(8)	1.165(8)	0.37	0.22			
	molecule-II	Core-I	2.074(8)	2.140(8)	0.41	0.06	6.35	36.1	3.61
		Core-II	2.061(8)	2.237(9)	0.36	0.20			

[a]Average value in Å. [b]Displacement (in Å) of Zn from the least-square plane of the $C_{20}N_4$ porphyrinato core. [c]Average displacement (in Å) of atoms from the least-square plane of the $C_{20}N_4$ porphyrinato core. [d]Nonbonding distance in Å. [e]Angle between two least-square plane of the $C_{20}N_4$ porphyrinato core. [f]Torsional angle.

Table S3. Calculated CD Spectral Data and Binding Constants of the Complexes at 295 K.

Compounds	FC[a]	SC[a]	A_{obs}[b] [cm^{-1} M^{-1}]	Binding Constant K_1 (M^{-1})[c,d]	FC[a]	SC[a]	A_{obs}[b] [cm^{-1} M^{-1}]	Binding Constant K_2 (M^{-1})[c,d]	Binding Constant K_3 (M^{-1})[c,d]
	1:1 complex, CD data λ (nm) [Δε, cm^{-1} M^{-1}]				2:3 complex, CD data λ (nm) [Δε, cm^{-1} M^{-1}]				
(1*S*, 2*S*)-CHDA	425[58]	410[-47]	105	$6.3 \pm 0.2 \times 10^5$ M^{-1} [$6.1 \pm 0.3 \times 10^5$ M^{-1}]	429[-87]	413[81]	-168	$2.0 \pm 0.1 \times 10^4$ M^{-1} [$1.7 \pm 0.2 \times 10^4$ M^{-1}]	$1.6 \pm 0.1 \times 10^4$ M^{-1} [$1.4 \pm 0.2 \times 10^4$ M^{-1}]
[(*S*)-PPDA]	425[43]	410[-35]	78	$8.7 \pm 0.1 \times 10^5$ M^{-1} [$8.2 \pm 0.2 \times 10^5$ M^{-1}]	427[-60]	413[57]	-117	$3.5 \pm 0.3 \times 10^4$ M^{-1} [$3.2 \pm 0.1 \times 10^4$ M^{-1}]	$1.4 \pm 0.3 \times 10^4$ M^{-1} [$1.0 \pm 0.1 \times 10^4$ M^{-1}]

[a]FC: 1st Cotton effect; [a]SC: 2nd Cotton effect. [b]*A*: total amplitude in M^{-1} cm^{-1}; $A = |\Delta\varepsilon_1 - \Delta\varepsilon_2|$ [c]Calculated from CD spectral measurement. [d]Value shown within the bracket are calculated from UV-visible spectral measurement.

Table S4. Selected Bond Lengths (Å) and Angles (deg) for DFT-optimized anticlockwise and clockwise oligomers of $\mathbf{1}_2$•[(1*S*, 2*S*)-CHDA]$_3$

Bond distance (Å)	Anticlockwise oligomer (molecule I)	Clockwise oligomer (molecule II)
Zn(1)-N(1)	2.115	2.103
Zn(1)-N(2)	2.060	2.096
Zn(1)-N(3)	2.077	2.059
Zn(1)-N(4)	2.107	2.115
Zn(1)-N(6)	2.229	2.175

Zn(2)-N(51)	2.106	2.112
Zn(2)-N(52)	2.059	2.064
Zn(2)-N(53)	2.100	2.075
Zn(2)-N(54)	2.100	2.091
Zn(2)-N(55)	2.235	2.260
Bond angle (º)		
N(1)-Zn(1)-N(2)	90.20	90.05
N(1)-Zn(1)-N(3)	157.65	161.99
N(1)-Zn(1)-N(4)	85.16	85.35
N(2)-Zn(1)-N(3)	87.46	87.05
N(2)-Zn(1)-N(4)	162.67	157.03
N(3)-Zn(1)-N(4)	90.51	90.41
N(51)-Zn(2)-N(52)	89.74	90.47
N(51)-Zn(2)-N(53)	161.82	157.31
N(51)-Zn(2)-N(54)	85.13	85.24
N(52)-Zn(2)-N(53)	86.25	87.04
N(52)-Zn(2)-N(54)	155.03	164.18
N(53)-Zn(2)-N(54)	91.06	91.07